Ultrawide-bandwidth, superluminescent light-emitting diodes using InAs quantum dots of tuned height

Haffouz, S.; Barrios, P. J.; Normandin, R.; Poitras, D.; Lu, Z.

Publisher's version / Version de l'éditeur:
https://doi.org/10.1364/OL.37.001103
OPTICS LETTERS, 37, 6, pp. 1103-1105, 2012-03-15

Ultrawide-bandwidth, superluminescent light-emitting diodes using InAs quantum dots of tuned height

S. Haffouz,* P. J. Barrios, R. Normandin, D. Poitras, and Z. Lu

Institute for Microstructural Sciences, National Research Council of Canada, Ottawa, Ontario, 1200 Montreal Road, M-50, K1A 0A6, Canada

**Corresponding author: sofiane.haffouz@nrc.ca*

Received November 9, 2011; revised January 26, 2012; accepted January 26, 2012; posted January 27, 2012 (Doc. ID 157837); published March 14, 2012

An ultrawide-bandwidth, superluminescent light-emitting diode (SLED) utilizing multiple layers of dots of tuned height is reported. Due to thermal effect, the superluminescent phenomenon is observed only under pulse-mode operation. The device exhibits a 3 dB bandwidth of 190 nm with central wavelength of 1020 nm under continuous-wave (cw) conditions. The maximum corresponding output power achieved in this device under cw and pulsed operation conditions are 0.54 mW and 17 mW, respectively. © 2012 Optical Society of America

OCIS codes: 160.6000, 230.3670, 230.5590, 250.5590, 250.5230.

One of the most attractive applications of superluminescent light-emitting diodes (SLEDs) as a light source has emerged after the successful demonstration of the optical coherence tomography (OCT) technique [1] and identification of its advantages compared to other imaging techniques in medical research and clinical practices. The performance characteristics of the light source in an OCT system such as central wavelength, bandwidth, output power, and spectral shape will directly affect the OCT image resolution. Moreover, for field application, compactness, stability, and overall cost of the OCT system should be considered. It has been demonstrated [2] that SLEDs operating at a central wavelength around 1060 nm offer the possibility to perform OCT imaging with better quality and deeper penetration in biological tissues due to the reduced loss and dispersion. SLEDs with extremely broad bandwidth are required in order to improve the image resolution in an OCT system. Although the highest axial resolution (1.8 μm in air) made by an OCT system operating at a central wavelength around 1 μm were so far achieved in research laboratories with a photonic crystal fiber—based source [3], SLEDs are considerably lower in cost and complexity.

It has been predicted that the natural large size inhomogeneity of the self-assembled quantum dots grown by the Stranski—Krastanow mode is very beneficial for broadening the gain spectra, which enhances the spectral width of the SLEDs. Sun *et al.* [4] reported that the full width at half maximum of the output spectrum of the $In_{0.9}Ga_{0.1}As/GaAs$ quantum dot (QD) system can be as high as 230 nm. Using five layers of InAs/GaAs QDs grown under identical growth conditions in a molecular beam epitaxy system, SLEDs with full width at half maximum of ~110 nm at a central wavelength of 1.1 μm have been made [5]. Further increasing the bandwidth of the emission spectrum of the SLEDs is a complicated process and requires more than just optimization of the growth conditions of the active region of the device. Using a thin capping $In_xGa_{1-x}As$ strain-reducing layer [6], QD-SLEDs with 121 nm bandwidth were demonstrated. By using an $Al_{0.14}Ga_{0.86}As$ barrier layer instead of GaAs, Lv *et al.* [7] demonstrated that the InAs dot size and distribution were significantly affected, which resulted in a light-emitting diode with a spectral bandwidth of 142 nm. Another successful approach was reported by Xin *et al.* [8] where they used a multiple-section SLED as a flexible device geometry that permits independent adjustment of the power and spectral bandwidth in the ground state and the excited states of the QD. An emission spectrum with full width at half maximum of 164 nm was achieved for a central wavelength of 1.15 μm. The maximum achieved output power in continuous-wave (cw) mode at this wavelength was about 0.6 mW. A bipolar cascade SLED [9] that uses tunneling junctions between distinct multiple quantum wells has resulted in an emitting device with spectral bandwidth of 180 nm at a central wavelength of 1.04 μm. The corresponding maximum cw output power was 0.65 mW.

In this Letter, we report on the demonstration of SLEDs operating at a central wavelength of 1020 nm where the active region of the device utilized multiple layers of InAs QDs of precisely tuned height from one layer to another. A 3 dB bandwidth as high as 190 nm was measured in cw operation mode.

The device structure was grown on an $n+$ GaAs (100) substrate in a solid-source V80H VG molecular beam epitaxy system. To achieve the 1 μm emission line, InAs QDs inside a GaAs matrix have been grown. The InAs material growth temperature and growth rate were 490 °C and 0.023 nm/s, respectively. The obtained dot density was $\sim 5\times10^{10}$ dots/cm^2. The active region of the device consisted of two repetitions of four layers of InAs quantum dots with GaAs barrier/cap layers of 30 nm thick, within a 300 nm waveguide. The InAs QDs were all deposited at 490 °C with the same amount of InAs materials (1.95 ML). 200 nm thick graded index $Al_xGa_{1-x}As$ ($x = 0.1$–0.33) layers were grown at 600 °C around the QD core with 1.5 μm $Al_{0.33}Ga_{0.67}As$:Be (1×10^{18} cm^{-3}) upper cladding and a 1.5 μm $Al_{0.33}Ga_{0.67}As$:Si (2×10^{18} cm^{-3}) lower cladding layer. After each 97 nm of n-cladding growth, a 3 nm GaAs:Si layer was grown to smooth the surface. The top 100 nm GaAs:Be contact layer was doped to a level of 2×10^{19} cm^{-3}, while the bottom GaAs:Si buffer layer was doped to 2×10^{18} cm^{-3}.

0146-9592/12/061103-03$15.00/0

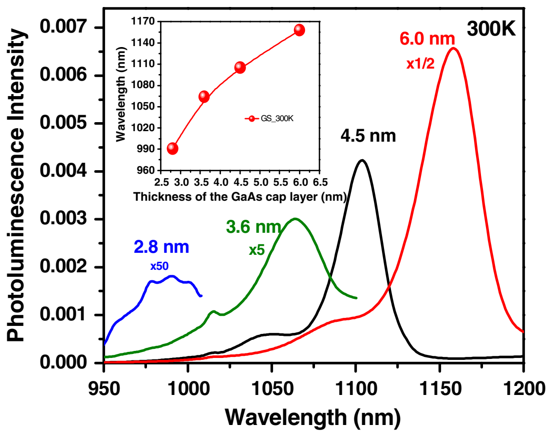

Fig. 1. (Color online) PL spectrum measured at room temperature of a single layer of dots where the In flush was executed after the deposition of a thin GaAs cap layer between 2.8 and 6.0 nm of thickness. The inset shows the variation of the ground-state (GS) emission wavelength as a function of the thickness of the GaAs cap layer.

The SLEDs were made in a tilted and tapered waveguide structure where the details of the device fabrication can be found in [10]. The device reported in this Letter was made with 1 mm long (L) waveguide and with tilted (α) and tapered (β) angles of 8° and 2°, respectively. The resulting width of the output facet was 35.49 μm. No facet coating was applied.

Tuning the dot height in the active region of the device structure was achieved using the In flush process [10,11], which consists in removing all surface-resident In at a certain position during the overgrowth of the GaAs cap layer. The In flush process was executed by interrupting the growth, rapidly raising the substrate temperature to 610 °C, and annealing for 70 s at that temperature. The deposited thicknesses at which the In flux was executed were 2.8 nm, 3.6 nm, 4.5 nm, and 6.5 nm starting from the bottom to top in the epitaxial device structure.

Figure 1 shows the photoluminescence (PL) spectrum measured at room temperature of a single layer of dots where the In flush was executed after the deposition of a thin GaAs cap layer between 2.8 and 6.0 nm of thickness. The PL intensity drop with decreasing the thickness of the GaAs cap layer was related to the reduction in the carrier confinement due to the reduced potential barrier for carriers in smaller dots. The inset of Fig. 1 shows the variation of the ground-state (GS) emission wavelength as a function of the thickness of the GaAs cap layer at which the In flush was executed. A redshift by 167 nm was obtained when the thickness of the GaAs layer was tuned from 2.8 nm to 6.0 nm. This implies that combining several layers of dots of tuned height in the active region of an SLED can be very beneficial in generating a broadband output emission spectrum.

Figure 2 shows the output power spectrum of the fabricated device as a function of the injection current under cw [Fig. 2(a)] and pulse mode operation [Fig. 2(b)]. The inset in Fig. 2(a) is a schematic drawing of the used waveguide. Increasing the cw injection current from 400 mA to 900 mA has resulted in extremely broadband and symmetric output emission spectra. At a drive current of 400 mA, a broadband emission centered on

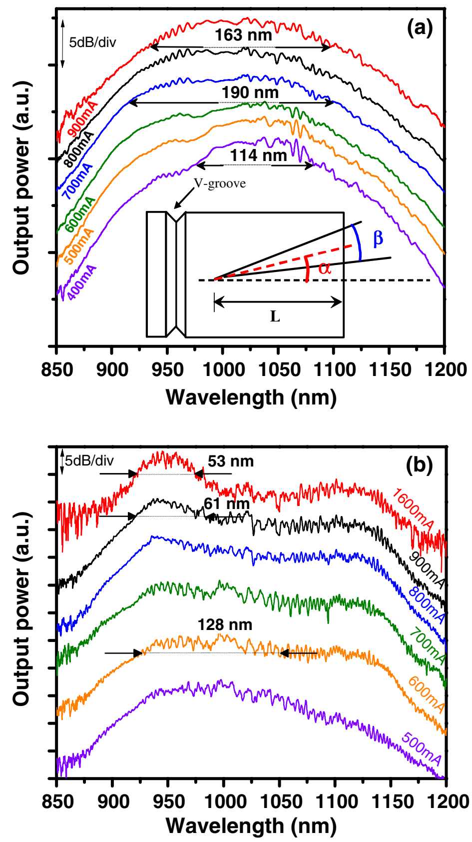

Fig. 2. (Color online) Emission spectra of the fabricated device at various injection current under (a) cw and (b) pulse operation mode with pulse width of 5 μs and duty cycle of 3%.

1033 nm with a bandwidth of 114 nm was obtained. By increasing the injection current up to 700 mA, the emission spectrum broadens further to reach 190 nm and the central wavelength blueshifted by only 10 nm to reach 1023 nm. Above an injection current of 700 mA, the central wavelength of the spectrum did not change, but we noticed bandwidth narrowing down to 163 nm at an injection current of 900 mA. This may indicate that at an injection current of 700 mA, all the energy levels (GS and excited states) of the different dots have been saturated and an emission spectrum fully represented by all dots' size distributions was achieved. However, above 700 mA, a disproportionate increase in gain for different wavelengths was taking place, resulting in spectral narrowing. Under pulse mode operation, a broadband spectrum with 3 dB bandwidth of 128 nm was measured at an injection current of 600 mA. Above this drive current, the bandwidth of the power spectrum decreases rapidly down to 53 nm at an injection current of 1600 mA.

Figure 3 shows the measured output power against the injection current (L-I) at 20 °C under cw and pulsed operation conditions. A maximum output power of 0.54 mW under 400 mA cw injection current was obtained. Above 400 mA, the output power decreased due to the thermal effects caused by high-series resistance as measured in our devices. An LED-like L-I curve was obtained. However, under pulsed mode, where the heating effect was minimized, a superlinear increase in output power was seen and a maximum output power of 17 mW was obtained with pulse width of 5 μs and duty cycle of 3%

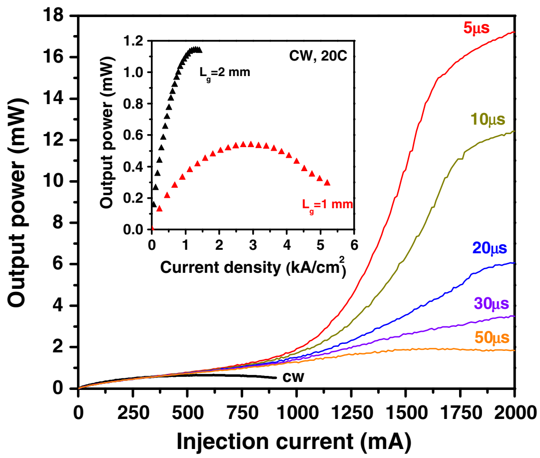

Fig. 3. (Color online) L-I curves measured under cw and pulsed operation conditions. The inset shows the output power versus the current density for 1 mm and 2 mm long devices measured at 20 °C under cw operation mode.

at an injection current of 2 A. Increasing the pulse width decreases the maximum achievable output power, but the superlinear behavior that starts above 1 A was observed in the L-I curve with a pulse width up to 50 μs.

We believe that the superlinear behavior in the L-I curve under cw mode is masked by the heating problem. Measurement of the L-I curves in different devices of 1 mm and 2 mm long demonstrated that the output power (see inset of Fig. 3) can significantly increase with increasing device length. This indicates that the single-pass amplification of the spontaneous emission generated along the waveguide did take place in our devices under cw operation conditions and it does vary with the cavity length.

In conclusion, we demonstrated ultrawide-bandwidth SLEDs using height-engineered InAs QDs. A calculated axial OCT resolution in air from the achieved 3 dB bandwidth of 190 nm at a central wavelength of 1020 nm was about 2.4 μm. This axial resolution is approaching that observed when using the state-of-the-art but bulky and expensive femtosecond laser source [3].

References

1. D. Huang, E. A. Swanson, C. P. Lin, J. S. Schuman, W. G. Stinson, W. Chang, M. R. Hee, T. Flotte, K. Gregory, C. A. Puliafito, and J. G. Fujimoto, Science **254**, 1178 (1991).
2. B. Povazay, B. Hermann, A. Unterhuber, B. Hofer, H. Sattmann, F. Zeiler, J. E. Morgan, C. Falkner-Radler, C. Glittenberg, S. Blinder, and W. Drexler, J. Biomed. Opt. **12**, 04211 (2007).
3. Y. Wang, Y. Zhao, J. S. Nelson, Z. Chen, and R. S. Windeler, Opt. Lett. **28**, 182 (2003).
4. Z.-Z. Sun, D. Ding, Q. Gong, W. Zhou, B. Xu, and Z.-G. Wang, Opt. Quantum Electron. **31**, 1235 (1999).
5. N. Liu, P. Jin, and Z.-G. Wang, Electron. Lett. **41**, 1400 (2005).
6. M. Rossetti, Li Lianhe, A. Markus, A. Fiore, L. Occhi, C. Velez, S. Mikhrin, I. Krestnikov, and A. Kovsh, IEEE J. Quantum Electron. **43**, 676 (2007).
7. X. Q. Lv, N. Liu, P. Jin, and Z. G. Wang, IEEE Photon. Technol. Lett. **20**, 1742 (2008).
8. Y.-C. Xin, A. Martinez, T. Saiz, A. J. Moscho, Y. Li, T. A. Nilsen, A. L. Gray, and L. F. Lester, IEEE Photon. Technol. Lett. **19**, 501 (2007).
9. S.-H. Guol, Jr.-H. Wang, Y.-H. Wu, W. Lin, Y. -J Yang, C.-K. Sun, C.-L. Pan, and J.-W. Shi, IEEE Photon. Technol. Lett. **21**, 328 (2009).
10. S. Haffouz, M. Rodermans, P. J. Barrios, J. Lapointe, S. Raymond, Z. G. Lu, and D. Poitras, Electron. Lett. **46**, 1144 (2010).
11. Z. R. Wasilewski, S. Fafard, and J. P. McCaffrey, J. Cryst. Growth **201/202**, 1131 (1999).